

Role of Carbonate Speciation on the Oxidation Rate of Fe(II) in Aquatic Systems

D. WHITNEY KING*

Department of Chemistry, Colby College,
Waterville, Maine 04901

A unified model for Fe(II) speciation and oxidation by molecular oxygen is described. This model combines Pitzer's concept of specific interaction with classic ion pair formation theory to describe ferrous iron speciation under conditions typical of natural waters. Using this model, it was determined that ferrous carbonate complexes [Fe(CO₃), Fe(CO₃)₂²⁻, and Fe(CO₃)(OH)⁻] dominate the speciation of Fe(II) in natural waters containing greater than 1 mM carbonate alkalinity. The speciation data were then utilized to evaluate the species-specific rates of Fe(II) oxidation by molecular oxygen for a range of media compositions and ionic strength. At pH values below 6.0, the oxidation rate of Fe(II) is well described in terms of the Fe²⁺ and FeOH⁺ species. However, for pH values above 6, the Fe(CO₃)₂²⁻ complex is the most kinetically active species. The combined speciation/oxidation model for Fe(II) was successful at predicting observed oxidation rates in lake water, well-defined salt solutions, and seawater.

Introduction

The redox cycling of iron in the environment plays a critical role in a range of biogeochemical processes including acid mine drainage, mineral solubility, catalysis of natural water oxidation reactions, and possibly iron limitation in the oceans. Increasingly, iron is being used as a photocatalyst for the oxidation of pesticides and herbicides in engineered systems (1). Essential to comprehending these complicated systems is a detailed mechanistic understanding of the electron-transfer reactions involved in Fe(III) reduction and Fe(II) oxidation. Since the first quantitative investigation of iron oxidation in natural waters was published by Stumm and Lee in 1961 (2) over 300 papers have been written on the rates and mechanism of Fe(II) oxidation in natural and engineered systems. The most detailed kinetic studies on Fe(II) oxidation were carried out by Millero and co-workers during the late 1980s (3-8). These works quantified the role of ionic strength and media composition on Fe(II) oxidation by oxygen and hydrogen peroxide over a range of temperatures. Critical to these works was the use of a consistent free hydrogen ion pH scale that facilitated intercomparison of rate data in varied media.

On the basis of both free energy calculations [e.g., Wehrli (9)] and studies that correlate the observed increases in the iron oxidation rate to the change in iron speciation with increased pH (e.g., Millero's work), it was determined that individual iron species react with different rates with oxygen. These authors have shown convincingly that the overall Fe-

(II) oxidation rate (k_{app}) can be explained in terms of the weighted sum of the oxidation rates of individual Fe(II) species:

$$-\frac{d\{\text{Fe(II)}\}}{dt} = [\text{O}_2]\{\text{Fe(II)}\}k_{app}$$

$$k_{app} = 4(k_1\alpha_{\text{Fe}^{2+}} + k_2\alpha_{\text{FeOH}^+} + k_3\alpha_{\text{Fe(OH)}_2^0} + \dots k_n\alpha_n) \quad (1)$$

where α_i is the fraction of each Fe(II) species in solution, k_i is the second-order rate constant for oxidation by oxygen, and $\{\text{Fe(II)}\}$ is the total or analytical Fe(II) concentration. The factor 4 in eq 1 reflects the stoichiometry of Fe(II) oxidation by oxygen when the first oxidation step is rate limiting (10, 11). Free hydrated Fe²⁺ has an oxidation half-life of days to weeks, while only trace quantities of highly reactive Fe(OH)₂⁰ can reduce the overall oxidation half-life to a few seconds. In contrast, kinetically less reactive species such as FeCl⁺ and FeSO₄⁰ must dominate Fe(II) speciation to significantly reduce oxidation rates. Clearly it is important to fully characterize ferrous iron speciation if one desires to adequately predict iron oxidation rates.

Recent improvements in Fe(II) speciation models (12) make detailed, species-dependent analysis Fe(II) oxidation rates practical. Of considerable interest with respect to this work was the prediction that carbonate complexes may dominate the inorganic speciation of Fe(II) in seawater and alkaline lake waters (12, 13). This domination may be responsible for the inability of Fe(II) oxidation models derived in controlled laboratory studies to adequately predict Fe(II) oxidation rates in seawater. It is possible that the order of magnitude overestimation of oxidation rates (θ) in seawater occurs because ferrous carbonate complexes were not considered.

In an attempt to provide a consistent model for Fe(II) oxidation over the full range of natural waters, we set out to reinvestigate the role carbonate ligands may play in Fe(II) oxidation. Carbonate is an important ligand in all natural waters and may form a variety of complexes with both Fe(II) and Fe(III). The effect of carbonate on Fe(II) oxidation was noted qualitatively in the early work of Stumm and Lee (2) and was studied quantitatively by Millero (6) and Ghosh (14). However, to date, no attempt has been made to fully explain these data in the context of Fe(II) speciation.

Experimental Section

Reagents. All solutions were prepared using 18 M Ω Nanopure water. Chemicals were reagent grade or better and were used as received. Ammonium ferrous sulfate hexahydrate and 5-amino-(2,3-dihydroxymethyl)aminomethane (luminol) were obtained from Fluka. Hydrochloric acid 30% suprapure and ammonia 25% suprapure were purchased from Merck.

Methods. The pH measurements were made using an Orion Ross electrode and an Orion meter calibrated on the free hydrogen ion scale using Tris buffers (15). Concentrations of Fe(II) were followed using an automated flow injection analysis system employing a luminol-based chemiluminescence detection of Fe(II) (11) modified by Emenegger et al. (10) to use 1 M NH₃ as the buffer in the luminol reagent. Oxygen solubility was calculated on the molal scale as a function of temperature and ionic strength using the data of Benson and Krause (16).

* Corresponding author phone: 207-872-3314; e-mail: dwking@colby.edu.

TABLE 1. Thermodynamic Constants for Fe(II) Speciation

no.	species	-log K at 25 °C		ref
		pure water	0.7 M NaCl	
1	H ₂ CO ₃ ⇌ HCO ₃ ⁻ + H ⁺	6.350	6.005	28
2	HCO ₃ ⁻ ⇌ CO ₃ ²⁻ + H ⁺	10.330	9.601	28
3	H ₂ O ⇌ H ⁺ + OH ⁻	13.995	13.710	28
4	Mg ²⁺ + OH ⁻ ⇌ MgOH ⁺	-2.19	-1.36	27
5	Mg ²⁺ + CO ₃ ²⁻ ⇌ MgCO ₃ ⁰	-2.98	-1.38	27
6	Fe ²⁺ + HCO ₃ ⁻ ⇌ FeHCO ₃ ⁺	-1.47	-0.97	27
7	Fe ²⁺ + CO ₃ ²⁻ ⇌ FeCO ₃ ⁰	-5.69	-4.33	13 ^a
8	Fe ²⁺ + 2CO ₃ ²⁻ ⇌ Fe(CO ₃) ₂ ²⁻	-7.45	-6.09	13 ^a
9	Fe ²⁺ + CO ₃ ²⁻ + OH ⁻ ⇌ Fe(CO ₃)(OH) ⁻	-9.97	-8.90	13 ^a
10	Fe ²⁺ + H ₂ O ⇌ FeOH ⁺ + H ⁺	9.51	9.66	12
11	Fe ²⁺ + 2H ₂ O ⇌ Fe(OH) ₂ ⁰ + 2H ⁺	20.61	20.87	12
12	Fe ²⁺ + Cl ⁻ ⇌ FeCl ⁺	-0.30	0.12	20 ^a
13	Fe ²⁺ + SO ₄ ²⁻ ⇌ FeSO ₄ ⁰	-2.42	-0.96	20 ^a

^a After reanalyses of the data as described in the text.

TABLE 2. Interaction Parameters for Activity Coefficient Calculations

species	Pitzer parameter, B ^p or β ^p	ref
H ⁺ , Na ⁺ , MgOH ⁺ , Mg ²⁺ , Cl ⁻ , OH ⁻ , HCO ₃ ⁻ , SO ₄ ²⁻ , CO ₃ ²⁻	full Pitzer, see supporting info	12
Fe ²⁺	full Pitzer, see supporting info ^a	27
FeCl ⁺ , FeOH ⁺ , FeHCO ₃ ⁺	0.22 ^b ; based on PbCl ⁺ ^a	29
Fe(CO ₃)(OH) ⁻	-0.19 ^b ; based on PbCl ₃ ⁻	29
MgCO ₃ ⁰	0.3188	27
FeCO ₃ ⁰	0.28	27
Fe(CO ₃) ₂ ²⁻	1.12	27
Fe(OH) ₂ ⁰	0.21; based on Cu(OH) ₂ ⁰	27
FeSO ₄ ⁰	0.3188 based on MgSO ₄	27

^a γ_{Fe²⁺}, and γ_{Fe^{x+}} in NaCl and Na₂SO₄ assumed equal to values in NaClO₄ at the same ionic strength. ^b β⁰ term.

Oxidation Experiments. Fe(II) oxidation experiments were performed in a 300-mL Pyrex water-jacketed beaker by adding a standard solution of Fe(II) to the O₂-saturated samples. The Fe(II) oxidation rates were investigated in a range of solutions including dilute carbonate, HEPES and PIPES buffers, and solutions containing added NaCl and Na₂SO₄ salts. For solutions buffered with carbonate, the pH was adjusted by bubbling a mixture of CO₂, N₂, and 20.9% O₂ through the system. Solutions buffered with HEPES and PIPES were sparged with pure air. In all cases the gas stream passed through a MnO₄⁻ solution to eliminate any H₂O₂. Solution temperatures were maintained at 25.0 ± 0.2 °C.

The initial Fe(II) concentrations for the oxidation experiments were 1–5 μM. These elevated Fe(II) concentrations were used to ensure that steady-state concentrations of O₂⁻, H₂O₂, and OH[•] were reached rapidly in all kinetic runs (11). Under these conditions, the reaction rate is first order with respect to Fe(II) and oxygen as described by eq 1. Oxygen was at considerable excess in all experiments. Values for k_{app} were obtained from first-order kinetic fits of Fe(II) concentration as a function of time over several half-lives. At the iron concentrations used in this study, autocatalysis of Fe(II) was not observed.

Speciation Calculations. Table 1 lists the thermodynamic constants used for speciation calculations in this work. Specific Fe(II) complexes considered are listed in reactions 6–13 in Table 1. We have adopted the mixed specific interaction/ion pairing approach of Millero (12) to model iron speciation. The activities of the major ions in solution (Na⁺, Mg²⁺, Cl⁻, SO₄²⁻, HCO₃⁻, CO₃²⁻) were calculated from their analytical concentrations, pH, and total activity coefficients calculated using Pitzer's specific interaction approach. In contrast, trace metal species were considered as distinct ion pairs. Stoichiometric association constants (K') for Fe(II) complexes were calculated from thermodynamic

constants in pure water (K) and appropriate activity coefficients (γ_i):

$$K' = K \frac{\lambda_M \lambda_X}{\lambda_{MX}} \quad (2)$$

Details on the specific interaction model used for activity coefficient calculations in this work are provided in the Supporting Information; and interaction parameters are listed in Table 2. Fe(II) is a trace species in all solutions which allows direct calculation of the fraction of Fe(II) species, α_{FeX}, in terms of the analytical ligand concentrations, [i], of all ligands and stoichiometric association constants:

$$\alpha_{Fe^{2+}} = 1 / (1 + \sum_i K'_i [i]) \quad (3)$$

$$\alpha_{FeX} = K'_X [X] \alpha_{Fe^{2+}} \quad (4)$$

In contrast to Millero (12), we chose to treat interactions between Fe(II) and chloride and sulfate as distinct FeCl⁺ and FeSO₄⁰ ion pairs. This approach is mechanistically more consistent with the observed acceleration and deceleration of Fe(II) oxidation rates in acidic and basic solutions respectively (6, 17–19). Values for the FeCl⁺ and FeSO₄⁰ association constants were calculated from the activity of Fe²⁺ in pure NaCl/Na₂SO₄ solutions (20). Equation 5 relates the activity of Fe²⁺ in terms of free and total concentrations and activity coefficients:

$$\alpha_{Fe^{2+}} = \gamma_f [Fe^{2+}] = \gamma_T \{ Fe^{2+} \} \quad (5)$$

where { } denote total concentrations, and γ_f and γ_T are free and total activity coefficients, respectively. Invoking FeCl⁺

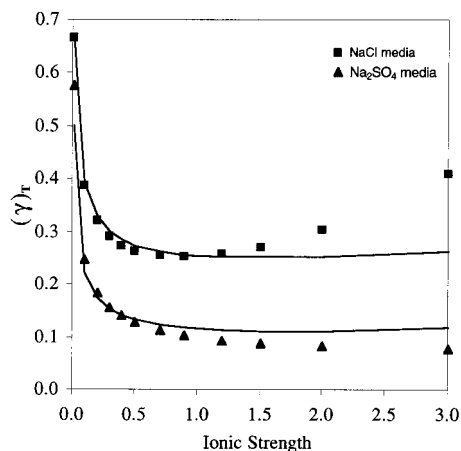


FIGURE 1. Total activity coefficient for Fe^{2+} in NaCl and Na_2SO_4 media. Symbols are γ_T values calculated with Pitzer equations assuming only specific interactions for $\text{Fe}^{2+}-\text{Cl}^-$ and $\text{Fe}^{2+}-\text{SO}_4^{2-}$. Curves are calculated γ_T values assuming the formation of FeCl^+ and FeSO_4^0 ion pairs.

and FeSO_4^0 ion pairs, the total concentration of Fe^{2+} is defined as

$$\{\text{Fe}^{2+}\} = [\text{Fe}^{2+}] + [\text{FeCl}^+] + [\text{FeSO}_4^0] \quad (6)$$

The ratio $[\text{Fe}^{2+}]/\{\text{Fe}^{2+}\}$ follows from eq 3:

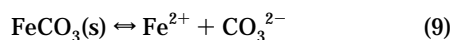
$$\frac{[\text{Fe}^{2+}]}{\{\text{Fe}^{2+}\}} = \frac{1}{(1 + K'_{\text{Cl}}[\text{Cl}^-] + K'_{\text{SO}_4}[\text{SO}_4^{2-}])} \quad (7)$$

Substitution of eq 5 into eq 7 provides an expression relating total activity coefficients to media composition, K'_i and γ_i :

$$\gamma_T = \gamma_i \frac{1}{(1 + K'_{\text{Cl}}[\text{Cl}^-] + K'_{\text{SO}_4}[\text{SO}_4^{2-}])} \quad (8)$$

Values for γ_i were obtained from activity measurements in noncomplexing media (NaClO_4) and are only a function of ionic strength. Figure 1 is a plot of the fit of eq 8 to total activity coefficient data. The values of $\log K'_{\text{FeCl}}$ and $\log K'_{\text{FeSO}_4}$ are listed in Table 1. These values are in good agreement with literature values for $\log K$ of 0.3 (21) and 2.2 (22) for chloride and sulfate, respectively.

Bruno et al. (13) have reported association constant values for ferrous carbonate species based on measurements of siderite solubility. These experiments were conducted in well-defined carbonate solutions at an ionic strength of 1 M. We have reanalyzed their data using activity coefficient values based on the interaction parameters of Millero and Hawke (27) (Table 2). Total Fe(II) solubility was then fit in terms of siderite solubility:



and three solution-phase side reactions (eqs 10–12) using the nonlinear Solver routine in Excel (Figure 2):

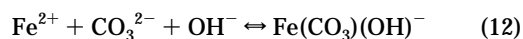


Table 1 lists the revised values for reactions 10–12. Our values for reactions 10 and 11 are in reasonable agreement

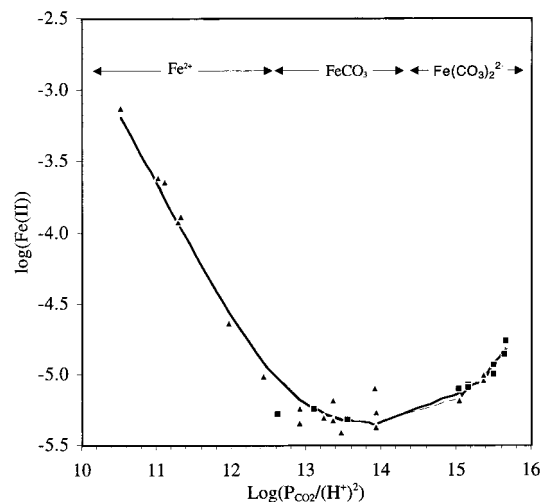


FIGURE 2. Siderite solubility data used to evaluate ferrous carbonate complexation. Symbols are experimental solubility data from Bruno et al. (13) measured at different p_{CO_2} ($\blacksquare = 0.01$, $\blacktriangle = 0.05$ atm). Solid and dashed lines are model fits including and excluding the $\text{Fe}(\text{CO}_3)(\text{OH})^-$ species, respectively. The dominant solution phase Fe(II) species are indicated above the data.

with Bruno's infinite dilution values of -5.5 and -7.1 for $-\log K_{\text{FeCO}_3}$ and $-\log K_{\text{Fe}(\text{CO}_3)_2}$, respectively. Slightly improved fits to the data were obtained if a third solution phase species, $\text{Fe}(\text{CO}_3)(\text{OH})^-$, was considered (Figure 2). Experimental evidence exists for a mixed $\text{Fe}(\text{III})(\text{CO}_3)(\text{OH})$ complex (23), but the $\text{Fe}(\text{II})(\text{CO}_3)(\text{OH})^-$ species has not been previously reported. Evidence for this species is supported indirectly from the modeling of Fe(II) oxidation rate data described below.

Figure 3 is the calculated inorganic Fe(II) speciation for conditions typical of lake water and seawater. The striking feature in this figure is the dominance of ferrous carbonate complexes above a pH of 7. Addition of Cl^- and SO_4^{2-} decreases the Fe^{2+} fraction by a factor of 2 and correspondingly shifts all other species by a comparable amount. Just the same, the ferrous carbonate species dominate Fe(II) speciation at the pH typical of seawater (8.2).

Results and Discussion

Figure 4 presents measured Fe(II) oxidation rates in carbonate, HEPES, and PIPES buffers at a pH of approximately 7.7. The complete data set is listed in Table 3. The Fe(II) oxidation rates in HEPES and PIPES show no dependence on buffer concentration, as compared to a strong dependence of Fe(II) oxidation rates on carbonate buffer concentration. These data are consistent with the formation of iron(II)–carbonate complexes that are oxidized rapidly by molecular oxygen.

To quantify these observations, the apparent first-order rate constant for each experiment was fit to a kinetic model described by eq 1. All nine species listed in Table 4 were considered as part of the fitting exercise:

$$k_{\text{app}} = 4(k_1\alpha_{\text{Fe}^{2+}} + k_2\alpha_{\text{FeCl}^+} + k_3\alpha_{\text{FeSO}_4^0} + k_4\alpha_{\text{FeOH}^+} + k_5\alpha_{\text{Fe}(\text{OH})_2^0} + k_6\alpha_{\text{Fe}(\text{HCO}_3)^+} + k_7\alpha_{\text{Fe}(\text{CO}_3)^0} + k_8\alpha_{\text{Fe}(\text{CO}_3)_2^{2-}} + k_9\alpha_{\text{Fe}(\text{CO}_3)(\text{OH})^-}) \quad (13)$$

However, many of these species are not present or can be ignored in the analysis of kinetic data for a specific experiment. Nonreactive species ($k \approx 0$) will essentially drop out of eq 13. Instead, their influence is manifested in decreased α terms for the reactive species. In the case of the HEPES

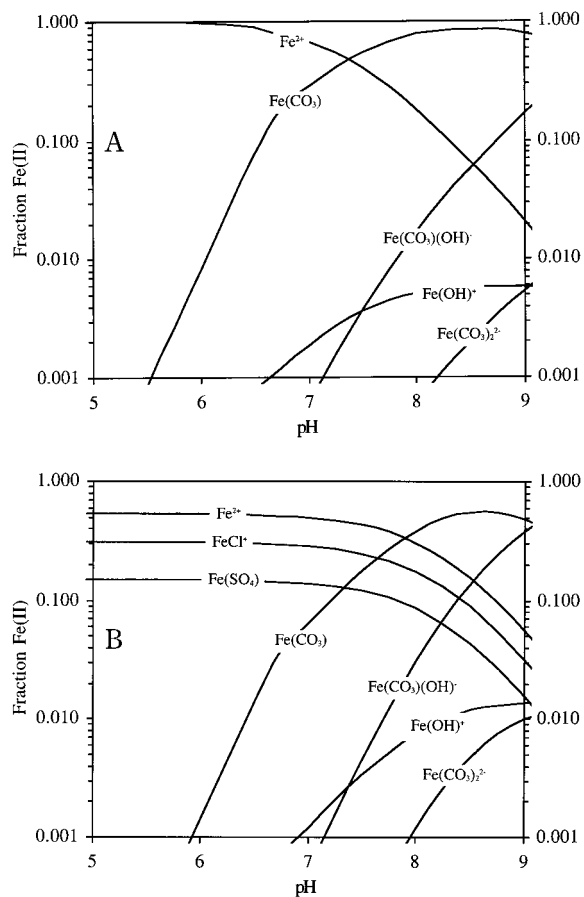


FIGURE 3. (A) Fe(II) speciation in pure water with 2.3 mM of NaHCO_3 and 0.03 atm of p_{CO_2} ; (B) Fe(II) speciation in 0.7 M of NaCl and 0.03 M of Na_2SO_4 with 2.3 mM of NaHCO_3 and 0.03 atm of p_{CO_2} .

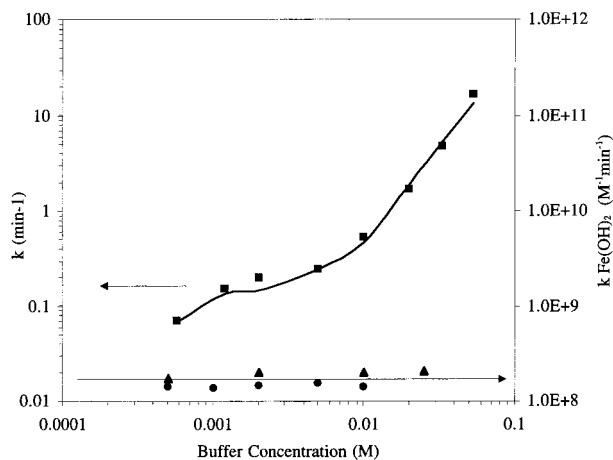


FIGURE 4. Observed and predicted Fe(II) oxidation rates as a function of buffer concentration at a pH of approximately 7.7. Specifics on solution composition and speciation are listed in Table 3. Symbols represent the following buffers: ■, bicarbonate; ▲, PIPES; and ●, HEPES. The left axis is the apparent first-order rate for oxygen-saturated bicarbonate solutions. The right axis is the second-order rate for Fe(OH)_2 oxidation by O_2 (k_5).

and PIPES, the model reduces to only one species (FeOH^+ was considered and can be ignored in this specific case):

$$k_{\text{app}} = 4\{k_5\alpha_{\text{Fe(OH)}_2^0}\} \quad (14)$$

Dividing k_{app} by calculated $\alpha_{\text{Fe(OH)}_2}$ allows calculation of k_5 . As shown in Figure 4, k_5 values are independent of buffer

concentration. This is expected since HEPES and PIPES buffers are noncomplexing, and minor ΔpH and ionic strength effects are accounted for in the $\alpha_{\text{Fe(OH)}_2}$ term.

A more complete model considering reactions k_5 – k_9 was used to fit the carbonate buffer data. This model was fit to all the data listed in Table 3. A necessary requirement for the model was that it fit the HEPES and PIPES data, the carbonate data shown in Figure 4, and rate data measured for carbonate buffers over a range of pH (6.9–8.3).

Values for k_5 – k_9 are also expected to have a dependence on ionic strength. Ionic strength effects are minor for these data sets as the ionic strength is low. However, estimates of the ionic strength dependence are necessary to extend the kinetic model to conditions typical of seawater or brines. Millero et al. (6) have made measurements of k_{app} for Fe(II) oxidation in carbonate buffered NaClO_4 media as a function of ionic strength. They fit the ionic strength dependence of k_{app} to the general form

$$\log k'_{\text{app}} = \log k_{\text{app}} + aI^{1/2} + bI \quad (15)$$

where k'_{app} is the apparent Fe(II) oxidation rate constant at an ionic strength I . For this work, we assumed that the ionic strength dependence of all rate constants (k_5 – k_9) can be described by an equation of the same form.

Our final modeling effort to estimate k_5 – k_9 used an iterative technique. We first fit our model to the data in Table 3 assuming an ionic strength of zero to obtain values for k_5 – k_9 . These values were then used as constants to fit a and b (eqn 15) to data obtained at high ionic strength. Estimates for a and b were then used to reevaluate k_5 – k_9 , and the process was repeated until the system converged.

Values for a and b are -1.338 and 0.5747 , respectively. Values for k_5 – k_9 are listed in Table 4. Ionic strength effects from 0 to 0.7 M decrease these rates by a factor of 5. Model fits are shown in Figures 4–6 and are listed in Table 3. The model fit is in very good agreement with experimental rate data. The exception is the fit to the pH 7.5 data in Figure 5. The trend in rate with ionic strength is well represented; however, initial rates are low by a factor of 25%. Comparison of the rates reveals that $\text{Fe(CO}_3)_2^{2-}$ is the principal species responsible for Fe(II) oxidation at $[\text{NaHCO}_3]$ above 2 mM. While the reaction rate for the Fe(OH)_2^0 species is the fastest by a factor of 100, the fraction of Fe(II) in this form is 200–500 times less than $\text{Fe(CO}_3)_2^{2-}$. The $\text{Fe(OH)(CO}_3)^-$ species showed intermediate reactivity, contributing about 20% to the overall Fe(II) oxidation rate. Due to the uncertainty in defining the equilibrium constant for this species and the minor influence the species contributed to the kinetic fits, the rate data for the $\text{Fe(OH)(CO}_3)^-$ species should be considered preliminary. The model was only able to provide upper estimates for k_6 and k_7 since FeHCO_3^+ and FeCO_3^0 exhibit slow oxidation kinetics making k_6 and k_7 poorly defined.

The above experiments were all performed at pH above 7.0. At lower pH values, oxidation of Fe^{2+} and Fe(OH)^+ species will become important. Figure 6 shows our fit to the k_{app} data of Singer and Stumm (24) using eq 14 with additional terms for Fe^{2+} and Fe(OH)^+ (k_1 and k_4). Agreement between experimental and modeled rates are excellent over the pH range of 2–6. Calculated values for k_1 and k_4 are listed in Table 4.

Figure 7 graphically presents our rate model in terms of Fe(II) species responsible for Fe(II) oxidation as a function of pH. The diagram clearly shows the importance of $\text{Fe(CO}_3)_2^{2-}$ species at the pH of most natural waters. This species is always a trace component in solutions below pH 8.5. However, due to the relatively large value of k_8 , the product $k_8\alpha_{\text{Fe(CO}_3)_2^{2-}}$ dominates the weighted sum of all Fe(II) species. The $\text{Fe(CO}_3)_2^{2-}$ species is also consistent with

TABLE 3. Fe(II) Oxidation Rates, Speciation, and Oxidation Model Fits for Bicarbonate, PIPES, and HEPES Buffers

buffer ^c	pH	log k ^d	speciation ^a							species rate ^b			log k (fit)	error ^f
			Fe ²⁺	Fe(OH) ⁺	Fe(OH) ₂	FeHCO ₃ ⁺	FeCO ₃	Fe(CO ₃) ₂ ²⁻	Fe(C) ^{-e}	Fe(OH) ₂	Fe(C) ⁻	Fe(CO ₃) ₂ ²⁻		
NaHCO ₃														
5.71E-04	7.387	-1.15	0.764	0.0056	1.06E-06	0.0115	0.218	9.10E-06	1.08E-03	0.0539	0.0094	0.0058	-1.15	0.01
1.20E-03	7.541	-0.82	0.537	0.0054	1.48E-06	0.0162	0.439	5.75E-05	3.19E-03	0.0731	0.0266	0.0355	-0.86	-0.05
2.00E-03	6.936	-1.61	0.726	0.0018	1.20E-07	0.0353	0.236	1.34E-05	4.36E-04	0.0058	0.0035	0.0081	-1.74	-0.14
2.00E-03	7.239	-1.35	0.585	0.0029	3.94E-07	0.0284	0.382	4.36E-05	1.42E-03	0.0189	0.0115	0.0261	-1.24	0.11
2.00E-03	7.239	-1.36	0.585	0.0029	3.94E-07	0.0284	0.382	4.36E-05	1.42E-03	0.0189	0.0115	0.0261	-1.24	0.12
2.00E-03	7.271	-1.38	0.568	0.0030	4.43E-07	0.0276	0.400	4.90E-05	1.59E-03	0.0213	0.0129	0.0294	-1.18	0.18
2.00E-03	7.516	-0.70	0.435	0.0040	1.05E-06	0.0211	0.536	1.16E-04	3.76E-03	0.0502	0.0305	0.0693	-0.82	-0.12
2.00E-03	8.057	0.02	0.184	0.0059	5.36E-06	0.0088	0.782	5.80E-04	1.91E-02	0.257	0.1540	0.3480	0.12	-0.14
2.00E-03	8.361	0.23	0.100	0.0065	1.18E-05	0.0048	0.846	1.25E-03	4.15E-02	0.567	0.3700	0.7480	0.22	-0.01
5.00E-03	7.475	-0.61	0.272	0.0022	5.19E-07	0.0299	0.691	3.78E-04	4.67E-03	0.0230	0.0350	0.2100	-0.57	0.04
1.00E-02	7.457	-0.28	0.177	0.0013	2.99E-07	0.0352	0.780	9.20E-04	5.39E-03	0.0122	0.0372	0.4690	-0.29	-0.01
2.00E-02	7.695	0.23	0.067	0.0008	3.22E-07	0.0233	0.893	4.24E-03	1.17E-02	0.0117	0.0714	1.92	0.30	0.07
3.33E-02	7.889	0.69	0.030	0.0006	3.41E-07	0.0155	0.921	1.29E-02	2.04E-02	0.0111	0.1120	5.23	0.73	0.04
5.33E-02	8.057	1.22	0.014	0.0004	3.41E-07	0.0104	0.908	3.43E-02	3.27E-02	0.0098	0.1570	12.2	1.09	-0.13
HEPES														
1.00E-03	7.692	-0.70	0.986	0.0140	5.46E-06					0.2741			-0.56	0.14
2.00E-03	7.687	-0.70	0.987	0.0135	5.21E-06					0.2508			-0.59	0.10
5.00E-03	7.714	-0.66	0.986	0.0137	5.62E-06					0.2490			-0.60	0.07
1.00E-02	7.686	-0.68	0.988	0.0122	4.71E-06					0.1905			-0.71	-0.03
PIPES														
5.00E-04	7.657	-0.67	0.987	0.0132	4.75E-06					0.2454			-0.60	0.06
2.00E-03	7.698	-0.55	0.986	0.0138	5.48E-06					0.2638			-0.57	-0.03
1.00E-02	7.618	-0.74	0.990	0.0105	3.45E-06					0.1395			-0.85	-0.11
2.50E-02	7.550	-0.90	0.992	0.0083	2.33E-06					0.0792			-1.09	-0.20

^a Fractional composition (α). ^b $\alpha_i k_i$. ^c Molal scale. ^d Units min^{-1} . ^e $\text{Fe}(\text{CO}_3)(\text{OH})^-$ species. ^f RMS error 0.10.

TABLE 4. Fe(II) Reaction Rates with Molecular Oxygen at 25 °C

	species	$l = 0 \log k^a$	$l = 0.7 \log k^b$	ref
1	$\text{Fe}^{2+} + \text{O}_2 \Rightarrow \text{Fe}^{3+} + \text{O}_2^-$	-4.26		24 ^c
2	$\text{FeCl}^+ + \text{O}_2 \Rightarrow \text{FeCl}^{2+} + \text{O}_2^-$			
3	$\text{FeSO}_4 + \text{O}_2 \Rightarrow \text{FeSO}_4^+ + \text{O}_2^-$			
4	$\text{Fe}(\text{OH})^+ + \text{O}_2 \Rightarrow \text{Fe}(\text{OH})^{2+} + \text{O}_2^-$	2.62		24 ^c
5	$\text{Fe}(\text{OH})_2 + \text{O}_2 \Rightarrow \text{Fe}(\text{OH})_2^+ + \text{O}_2^-$	7.72	7.00	<i>d</i>
6	$\text{FeHCO}_3^+ + \text{O}_2 \Rightarrow \text{FeHCO}_3^{2+} + \text{O}_2^-$	<1.9		<i>d</i>
7	$\text{FeCO}_3 + \text{O}_2 \Rightarrow \text{FeCO}_3^+ + \text{O}_2^-$	<1.4		<i>d</i>
8	$\text{Fe}(\text{CO}_3)_2^{2-} + \text{O}_2 \Rightarrow \text{Fe}(\text{CO}_3)_2^- + \text{O}_2^-$	5.82	5.10	<i>d</i>
9	$\text{Fe}(\text{CO}_3)(\text{OH})^- + \text{O}_2 \Rightarrow \text{Fe}(\text{CO}_3)(\text{OH}) + \text{O}_2^-$	4.0	3.2	<i>d</i>

^a $\text{M}^{-1} \text{min}^{-1}$, calculated from $k/4$. ^b Calculated using eq 15. ^c After reanalyses of the data as described in the text. ^d This work.

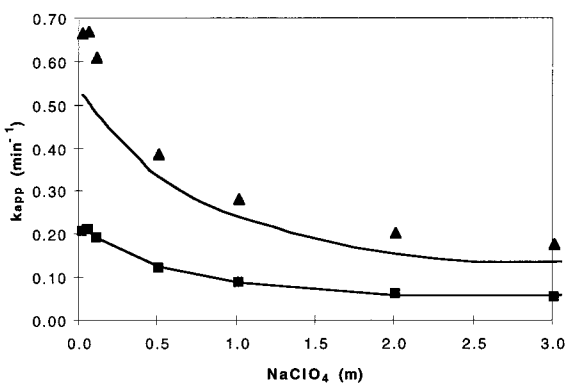


FIGURE 5. Ionic strength dependence on k_{app} and model fits. Symbols are from Millero et al. (δ) (pH 7.25 = \blacksquare and pH 7.5 = \blacktriangle), and solid lines are model fits.

second-order OH^- dependence on Fe(II) oxidation reported by many investigators (2, 3, 10, 25). The $\text{p}K_a$ of HCO_3^- is 10.3 so that below pH 8.8 the $[\text{CO}_3^{2-}]$ is first-order with respect to $[\text{OH}^-]$. Consequently, the iron(II)-biscarbonate complexes will be second-order with respect to $[\text{OH}^-]$. The nearly first-order carbonate dependence on Fe(II) oxidation rate (Figure 4) is also consistent with the FeCO_3 being the major

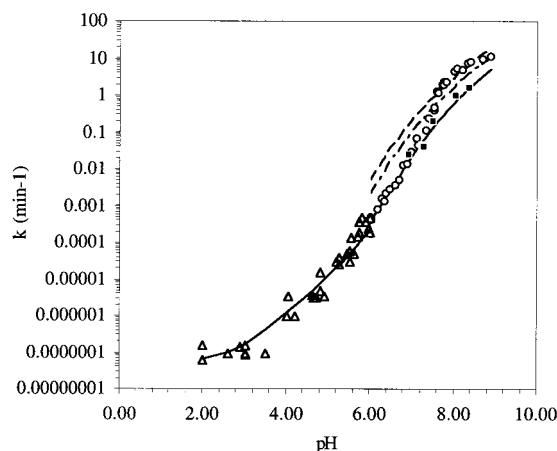


FIGURE 6. Effect of pH and carbonate on oxidation rate. Lines are modeled rates for 2, 9, and 16 mM NaHCO_3 moving from bottom to top, respectively. Symbols are experimental data: \circ = Millero et al. (δ) (9 mM of NaHCO_3), \blacksquare = this work (2 mM of NaHCO_3), \triangle = Singer and Stumm (24).

Fe(II) species above pH 7.25 where oxidation rates are controlled by the trace $\text{Fe}(\text{CO}_3)_2^{2-}$ species ($\alpha_{\text{Fe}(\text{CO}_3)_2}$ is proportional to $[\text{CO}_3^{2-}]$).

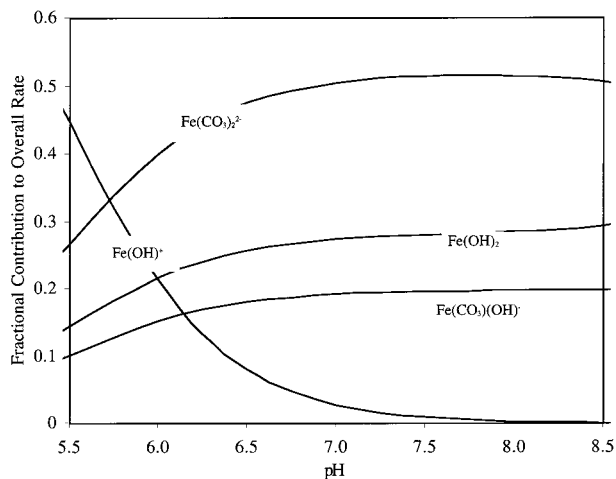


FIGURE 7. Contribution of specific Fe(II) species in total Fe(II) oxidation rate by O_2 . Calculations are for pure water with 2.3 mM $NaHCO_3$ at 25 °C.

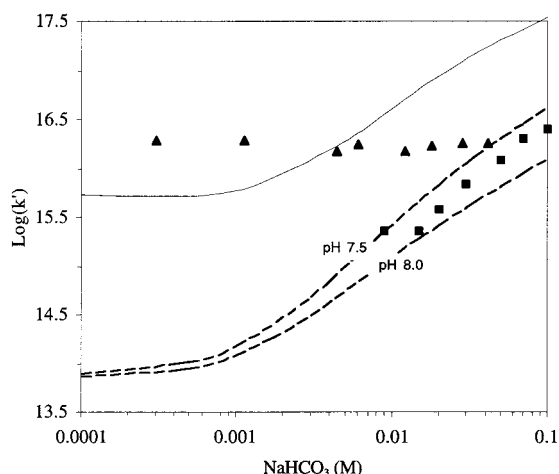


FIGURE 8. Comparison of published rates ($k' = k_{app}/[OH^-][O_2]$) with model predictions as a function of carbonate buffer concentration. [■ from Millero and Izaguirre (6) (1 M NaCl, pH 7.5), ▲ from Ghosh (14) (pure water, pH 6.8), lines are model predictions (solid for Ghosh, dashed for Millero)].

As a test of our complete kinetic model for Fe(II) oxidation, we compared our model predictions for Fe(II) oxidation rate with experimental data obtained in pure water and simple salt solutions (Figures 6, 8, and 9). Our predicted rates parallel Millero's pure water data at most pH values but overestimate the rate below pH 7.5 and underestimate the rate above pH 7.8 (Figure 6). In general, the agreement is really quite good, and slight variations in solution carbonate concentration may explain the differences. Notice that the model fits have a slope ($\log k$ vs pH) approaching 2, but they show considerable curvature at higher pH values. The curvature is a consequence of the pH dependence on the $Fe(CO_3)_2^{2-}$ species. This curvature is also observed in the experimental data. Comparing our model to previous investigations of carbonate effects, our data agree well with the Millero and Izaguirre data measured in 1 M NaCl solutions (Figure 8), while the discrepancy with the Ghosh data cannot be adequately explained. The modeled curves (Figure 8) also provide a general sense of the sensitivity of Fe(II) oxidation rates to carbonate concentration. Below an alkalinity of 1 mM carbonate effects are minor, while above 1 mM the increase in oxidation rate is linear with carbonate concentration.

Finally, the effect of Na^+ , Mg^{2+} , and Cl^- ions on carbonate buffered solutions is shown in Figure 9. These experiments

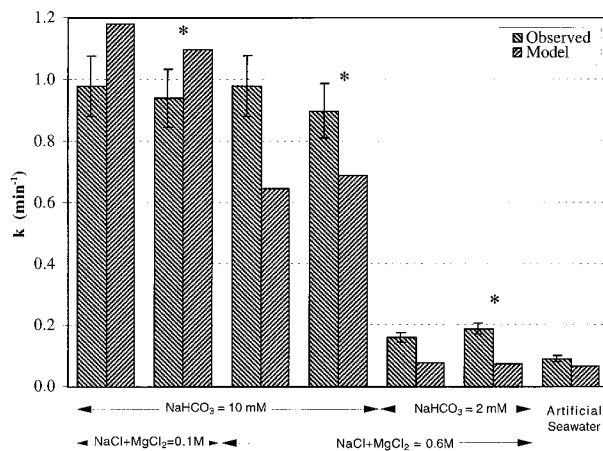


FIGURE 9. Comparison of rates in different media. (pH 7.75, left diagonal experimental data, right diagonal model fit). The asterisk (*) indicates data with 50 mM $MgCl_2$ added. The experimental rate for artificial seawater is from ref. 6.

were conducted to investigate the role that cations may play in influencing Fe(II) oxidation rates. Experimental and modeled rates agree within 20%. Carbonate concentrations have the largest effect on oxidation rates. Addition of chloride reduced rates to a moderate extent due to increasing ionic strength and chloride complexation of Fe(II) ($k_2 \approx 0$). In contrast to the observation of previous investigators (6), the addition of Mg^{2+} had no effect on the observed rates. The Fe(II) oxidation rate in artificial seawater is also well predicted by the kinetic model. In this solution, chloride and sulfate complexation of Fe(II) and increased ionic strength are the significant processes responsible for reduced rates as compared to pure water.

Significance of Results

A chemical model for Fe(II) oxidation has been developed that accurately describes the oxidation rate of Fe(II) by oxygen as a function of pH and media composition (pure water to seawater). The model is consistent with the experimental rate measurements reported in this work and the vast majority of literature values. While several studies have modeled Fe(II) oxidation rates in terms of species specific reactivity (9, 26), this is the first time that a single model could explain Fe(II) oxidation rates over the full compositional range of natural waters.

The results of a mixed specific interaction/ion-pairing model for Fe(II) speciation show that the $FeCO_3^0$ species dominates the inorganic speciation of Fe(II) at circumneutral pH. In contrast, the rate of Fe(II) oxidation is controlled by a trace species, $Fe(CO_3)_2^{2-}$. The first hydrolysis product of iron, $Fe(OH)^+$, is important in establishing Fe(II) oxidation rates in acid media. However, the $Fe(OH)_2^0$ species is much less important than previously thought in solutions containing millimolar levels of carbonate typical of many natural waters.

The recent work by Emmenegger et al. (10) showed that Fe(II) oxidation in lake water is consistent with this model at a pH above 7.5 but showed a marked acceleration at lower pH due to a possible Fe(II) ligand. The utility of our Fe(II) oxidation model is that it provides a reference point in which to evaluate Fe(II) oxidation by O_2 in natural waters where organic ligands and surfaces may accelerate or decelerate rates. A comprehensive model for Fe(II) oxidation will not be complete, however, until a comparable study using an updated speciation model is performed for Fe(II) oxidation by hydrogen peroxide. The limited data available indicates that $k_{H_2O_2}$ at pH 6 increases with a near first-order dependence with $NaHCO_3$ concentration (4). These data suggest that an

iron(II)–monocarbonate species may be the kinetically reactive form of Fe(II) for oxidation by hydrogen peroxide. Preliminary analysis would suggest the $\text{Fe}(\text{CO}_3)_0$ species as the reactive Fe(II) complex. Additional experiments at elevated pH and in the absence of carbonate will be needed to confirm these speculations.

Acknowledgments

Financial support was provided by the William and Flora Hewlett Foundation Award of the Research Corporation and the Maine NASA Space Grant Consortium. The tremendous hospitality of Dr. Barbara Sulzberger and Prof. Laura Sigg while the author was on sabbatical at EAWAG was greatly appreciated. Insightful comments and suggestions by Prof. Werner Stumm and Lukas Emmenegger over the course of this work were greatly appreciated.

Supporting Information Available

An estimation of activity coefficients and β^0_{mx} , β^1_{mx} , β^2_{mx} , C^{ϕ}_{mx} , Φ_{cc} , Φ_{as} , Ψ_{ccCl} , Ψ_{ccSO_4} , Ψ_{aaNa} , and Ψ_{aaMg} terms (9 pages). Ordering information is given on any current masthead page.

Literature Cited

- (1) Pignatello, J. J.; Baehr, K. *J. Environ. Qual* **1994**, *23*, 365–370.
- (2) Stumm, W.; Lee, G. F. *Ind. Eng. Chem.* **1961**, *53*, 143–146.
- (3) Millero, F. J.; Sotolongo, S.; Izaguirre, M. *Geochim. Cosmochim. Acta* **1987**, *51*, 793–801.
- (4) Millero, F. J.; Sotolongo, S. *Geochim. Cosmochim. Acta* **1989**, *53*, 1867–1873.
- (5) Millero, F. J. *Mar. Chem.* **1989**, *28*, 1–18.
- (6) Millero, F. J.; Izaguirre, M. *J. Solution Chem.* **1989**, *18*, 585–599.
- (7) Millero, F. J. *Mar. Chem.* **1990**, *30*, 205–229.
- (8) Millero, F. J. In *Chemical Modeling of Aqueous Systems II*; Melchior, D. C., Bassett, R. L., Eds.; American Chemical Society: Washington, DC, 1990; pp 447–460.
- (9) Wehrli, B. In *Aquatic Chemical Kinetics*; Stumm, W., Ed.; Wiley: New York, 1990; pp 311–37.
- (10) Emmenegger, L.; King, D. W.; Sigg, L.; Sulzberger, B. *Environ. Sci. Technol.* **1998**, *32*, 0000–0000.
- (11) King, D. W.; Lounsbury, H. A.; Millero, F. J. *Environ. Sci. Technol.* **1995**, *29*, 818–824.
- (12) Millero, F. J.; Yao, W.; Archer, J. *Mar. Chem.* **1995**, *50*, 21–39.
- (13) Bruno, J.; Wersin, P.; Stumm, W. *Geochim. Cosmochim. Acta* **1992**, *56*, 1149–1155.
- (14) Ghosh, M. M. In *Aqueous-Environmental Chemistry of Metals*; Rubin, A. J., Ed.; Ann Arbor Science: Ann Arbor, 1974; pp 193–217.
- (15) Millero, F. J.; Hershey, J. P.; Fernandez, M. *Geochim. Cosmochim. Acta* **1987**, *51*, 707–711.
- (16) Benson, B. B.; Daniel Krause, J. *Limnol. Oceanogr.* **1984**, *29*, 620–632.
- (17) Matseevskii, B. P.; Chernaya, S. S. *Latv. PSR Zinat. Akad. Vestis. Kim. Ser.* **1980**, *4*, 439–44.
- (18) Sung, W.; Morgan, J. J. *Environ. Sci. Technol.* **1980**, *14*, 561–568.
- (19) Tamura, H.; Goto, K.; Nagayama, M. *J. Inorg. Nucl. Chem* **1976**, *38*, 113–17.
- (20) Pitzer, K. S. In *Activity Coefficients in Electrolyte solutions*; Pitzer, K. S., Ed.; CRC Press: Boca Raton, FL, 1991; pp 75–153.
- (21) Kester, D. R.; Byrne, R. H.; Liang, Y.-J. In *Marine Chemistry in the Coastal Environment*; Church, T. M., Ed.; ACS Symposium Series 18; American Chemical Society: Washington, DC, 1975; pp 56–79.
- (22) Wells, C. F. *J. Chem. Soc.* **1968**, 308.
- (23) Bruno, J.; Stumm, W.; Wersin, P.; Brandenberg, F. *Geochim. Cosmochim. Acta* **1992**, *56*, 1139–1147.
- (24) Singer, P. C.; Stumm, W. *Science* **1970**, *167*, 1121–1123.
- (25) Davidson, W.; Seed, G. *Geochim. Cosmochim. Acta* **1983**, *47*, 793–801.
- (26) Millero, F. J. *Mar. Chem.* **1990**, *30*, 205–29.
- (27) Millero, F. J.; Hawke, D. J. *Mar. Chem.* **1992**, *40*, 19–48.
- (28) Millero, F. J. *Geochim. Cosmochim. Acta* **1995**, *59*, 661–677.
- (29) Millero, F. J.; Byrne, R. H. *Geochim. Cosmochim. Acta* **1984**, *48*, 1145–50.

Received for review March 3, 1998. Revised manuscript received June 24, 1998. Accepted June 26, 1998.

ES980206O